Fold and thrust systems in mass transport deposits around the Dead Sea Basin

Article *in* Geophysical Monograph Series · May 2018

CITATIONS
3

READS
250

4 authors, including:

G. I. Alsop
University of Aberdeen
186 PUBLICATIONS **3,381** CITATIONS
SEE PROFILE

Ram Weinberger
Geological Survey of Israel
112 PUBLICATIONS **1,633** CITATIONS
SEE PROFILE

Shmuel Marco
Tel Aviv University
173 PUBLICATIONS **947** CITATIONS
SEE PROFILE

Geophysical Monograph 246

Submarine Landslides
Subaqueous Mass Transport Deposits from Outcrops to Seismic Profiles

Kei Ogata
Andrea Festa
Gian Andrea Pini
Editors

This Work is a co-publication of the American Geophysical Union and John Wiley and Sons, Inc.

AGU 100
ADVANCING EARTH AND SPACE SCIENCE

WILEY

9

Fold and Thrust Systems in Mass-Transport Deposits Around the Dead Sea Basin

G. Ian Alsop[1], Rami Weinberger[2,3], Shmuel Marco[4], and Tsafrir Levi[2]

ABSTRACT

The late Pleistocene Lisan Formation outcropping around the Dead Sea preserves exceptional 3D exposures of fold and fault systems generated during soft-sediment slumping associated with mass-transport deposits (MTDs). Vergence of slump folds outcropping to the west of the Dead Sea is generally (>90%) toward the east and consistent with depocenter-directed movement of MTDs. On a regional scale, the direction of slumping inferred from the fold and thrust geometries systematically varies along the entire ~100 km length of the western Dead Sea Basin. The fold and thrust systems are interpreted to form part of a large-scale radial system of MTDs directed toward the basin's depocenter and to be triggered by earthquakes generated along the Dead Sea Fault. The progressive evolution of MTDs is broadly categorized into initiation, translation, cessation, relaxation, and compaction phases. Deformation may become most evolved where slope failure initiates and MTD movement commences. Consequently, many MTDs display the greatest deformation in their central area, and this diminishes toward the leading edge where MTD displacement was still initiating. Thrust packages may define piggyback sequences during MTD translation, while in other cases, overstep thrust sequences are formed, leading to a range of crosscutting and overprinting relationships. The recognition that MTDs may be reworked by younger seismically triggered events suggests that in some cases, the seismic recurrence interval may be shorter than anticipated. Our observations of heterogeneous lateral compaction, together with upright folding that represents an early phase of layer-parallel shortening, may help explain why some contraction is apparently missing from seismic sections across large-scale MTDs. In addition, conjugate normal faults that strike parallel to the dip of the paleoslope indicate a component of non-plane strain deformation associated with "out-of-plane" movement. MTDs in the Dead Sea Basin are best described as having open-ended toes (a variant of frontally confined toes) in which further movement is impeded by downslope strata that form a "soft" buttress. Observations that contraction and extension may overprint one another at any position within an MTD suggest that second-order flow cells may locally interact with one another and are linked to "pockets" of "surging" or "slackening" flow during overall downslope translation of the MTD. The spacing of thrust ramps within MTDs are linearly related to the thickness of the section to define an approximate 5 : 1 ratio across a range of scales. In summary, the MTDs in the Lisan Formation exposed around the Dead Sea Basin are triggered by seismic events, may be facilitated by mechanical heterogeneity linked to detrital-rich horizons, and are ultimately controlled by the paleoslope orientation.

[1] *Department of Geology and Geophysics, School of Geosciences, University of Aberdeen, Aberdeen, United Kingdom*

[2] *Geological Survey of Israel, Jerusalem, Israel*

[3] *Department of Geological and Environmental Sciences, Ben Gurion University of the Negev, Beer Sheva, Israel*

[4] *Department of Geophysics, Tel Aviv University, Tel Aviv-Yafo, Israel*

9.1. INTRODUCTION AND REGIONAL SETTING OF MTDS IN THE DEAD SEA BASIN

The Dead Sea Basin is a pull-apart basin formed between two sinistral and left-stepping fault strands that comprise the Dead Sea Fault (Figure 9.1a) (e.g., Garfunkel,

Submarine Landslides: Subaqueous Mass Transport Deposits from Outcrops to Seismic Profiles, Geophysical Monograph 246, First Edition. Edited by Kei Ogata, Andrea Festa, and Gian Andrea Pini.

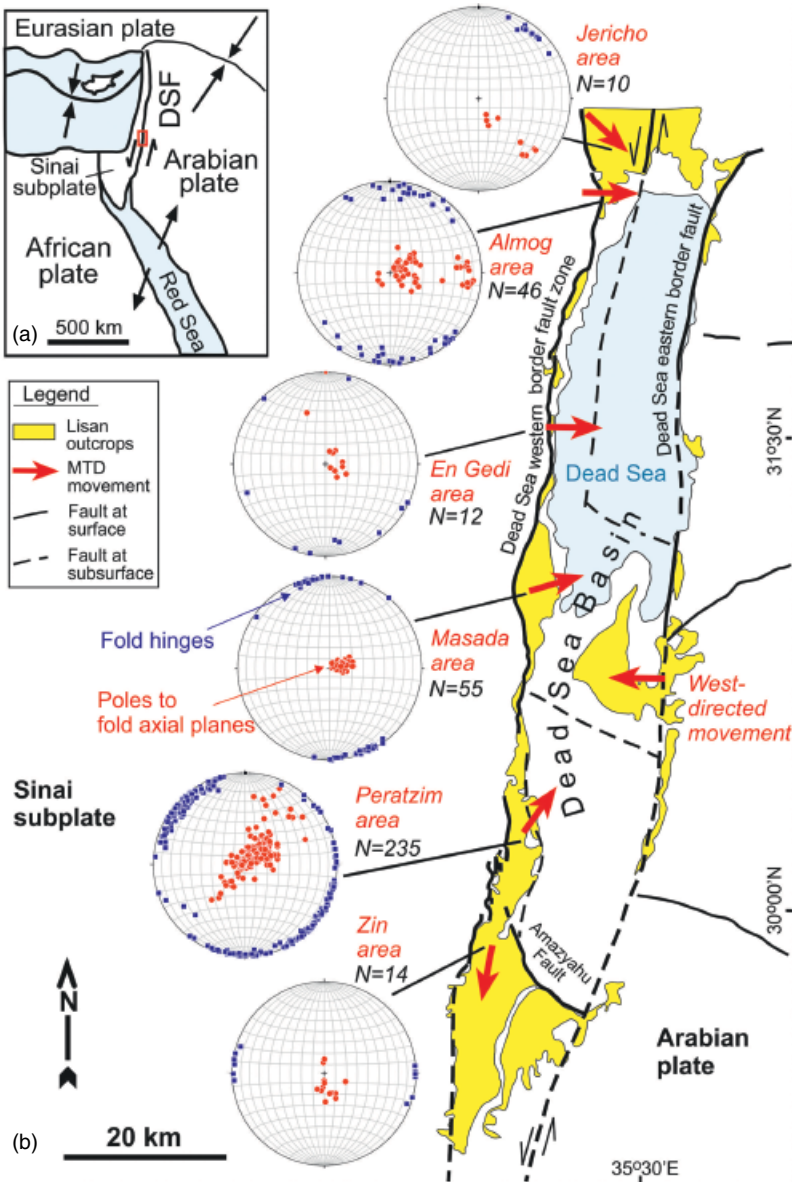

Figure 9.1 (a) General tectonic map of the Middle East showing the location of study area (red box) along the Dead Sea Fault (DSF). The DSF transfers the opening motion in the Red Sea to the Taurus-Zagros collision zone. (b) Map of the Dead Sea showing the position of localities referred to in the text and the extent of the Lisan Formation outcrops. Stereonets show fold hinges (blue squares) and poles to axial planes (red circles) that have been measured from slump folds within MTDs of the Lisan Formation. The red arrows represent the inferred direction of MTD movement within the Lisan Formation and form a semi-radial pattern centered around the Dead Sea Basin. Westerly directed movement along the eastern margin of the basin is based on El-Isa and Mustafa (1986). (*See electronic version for color representation of this figure*)

1981, 2014; Sneh and Weinberger, 2014). The Dead Sea Fault forms a transform boundary that has been active since the early to middle Miocene (e.g., Nuriel et al., 2017), including during the late Pleistocene when the Lisan Formation was deposited between 70 and 15 ka in a precursor lake to the Dead Sea (Haase-Schramm et al., 2004). Numerous earthquakes have been triggered by the Dead Sea Fault, resulting in coseismic deformation (e.g., Agnon et al., 2006; Weinberger et al., 2016), together with soft-sediment deformation and mass-transport deposits (MTDs) in the Lisan Formation (El-Isa and Mustafa, 1986; Marco et al., 1996; Alsop and Marco, 2011). It is these MTDs that are exceptionally well exposed in outcrops of the Lisan Formation around the Dead Sea

Basin that form the focus of this study (Marco et al., 1996; Alsop et al. 2016). The MTDs that we describe are generally no more than a few meters thick, with constraints of continuous exposure limiting our ability to trace them along strike for ~500 m, and downslope for a few kilometers, suggesting overall volumes for individual MTDs of <0.5 km^3. However, larger MTDs exist, as significant numbers of deformed horizons have been recovered from cores through the Lisan Formation in the depocenter of the Dead Sea Basin (Lu et al., 2017; Kagan et al. 2018).

Coseismic slip along bedding planes in the Lisan Formation results in horizontal offset of vertical clastic dikes and is created by seismic waves generated by earthquakes passing through the sediment (Weinberger et al., 2016). Such seismic events are also thought to trigger older MTDs within the Lisan Formation, where topography created in the hanging wall of normal faults is infilled by breccia formed during the same seismic event (e.g., El-Isa and Mustafa, 1986; Marco et al., 1996; Alsop and Marco, 2011). A recent discussion of the seismic origin of MTDs within the Lisan Formation is provided by Lu et al. (2017). Following the initial seismic event that triggers slope failure, MTDs then undergo gravity-driven downslope movement toward the depocenter of the basin (Alsop and Marco, 2012a). Multiple MTDs that are transported into the center of the basin have resulted in a threefold thickening of the Lisan Formation where penetrated by drill cores (Lu et al., 2017; Kagan et al., 2018). Thus, although slope failure is triggered by an earthquake which perhaps lasts in the order of seconds (e.g., see Shani-Kadmiel et al., 2014), subsequent downslope movement of MTDs generates the observed fold and thrust systems and is gravity driven. This downslope movement of MTDs is completed prior to deposition of an overlying sedimentary "cap" that settles out of suspension, potentially "in a matter of just hours or days" (Alsop et al., 2016, p. 80).

The Lisan Formation comprises a sequence of alternating aragonite-rich and detrital-rich laminae on a submillimeter scale. Aragonite-rich laminae are considered to precipitate from hypersaline waters in hot dry summers, while winter floods wash detrital sediment into the lake to create annual varve-like cycles (Begin et al., 1974). Detrital laminae within the varved aragonite-rich Lisan Formation consist of quartz and calcite grains with minor feldspar, and clays (illite-smectite), and display grain sizes of ~8–10 μm (silt), while the thicker detrital-rich units are classified as very fine sands (60–70 μm) (Haliva-Cohen et al., 2012). The sedimentation rate of the Lisan Formation is estimated from varve counting combined with isotopic dating and is thought to average ~1 mm/year (Prasad et al., 2009). These exceptional layer-cake stratigraphies, developed on a centimeter scale within the lacustrine environment, potentially provide numerous easy-slip horizons to facilitate translation of the MTDs.

The Lisan Formation was deposited on very gentle slopes of <1° (Alsop and Marco, 2013). MTDs that move down very low angle slopes are frequently reported in the literature (e.g., Lewis, 1971; Almagor and Garfunkel, 1979; Gibert et al., 2005; Garcia-Tortosa et al., 2011; Gladkov et al., 2016), with modern failures recorded on gradients as low as 0.25° (e.g., Wells et al., 1980; Field et al., 1982). Hence, the very gentle slopes developed in the Lisan Formation should not be considered too low or insufficient to drive downslope movement, as supported by analogue experiments that demonstrate that such low gradients are capable of driving sediment deformation (e.g., Owen, 1996). Within the Lisan Formation, failure and translation of MTDs on very gentle slopes (<1°) may be facilitated by pore fluid pressure (e.g., Arkin & Michaeli, 1986) that is increased during seismicity and also loading associated with translation of MTDs themselves (Alsop et al., 2018).

This study aims to review a number of factors pertaining to MTDs around the Dead Sea Basin, which may also have more general relevance:

1. Analyzing regional patterns of MTD movement around the Dead Sea Basin
2. Analyzing structural sequences during internal evolution of MTDs
3. Analyzing reworking triggered by multiple seismic events within MTDs
4. Analyzing contractional structures that are hidden on seismic images
5. Analyzing the external geometry of MTDs around the Dead Sea Basin

9.2. ANALYZING REGIONAL PATTERNS OF MTD MOVEMENT AROUND THE DEAD SEA BASIN

The careful measurement of slump fold orientation has long been used to infer the direction of paleoslopes (e.g., Woodcock, 1976a, 1976b, 1979; Korneva et al., 2016; Jablonska et al., 2018). Detailed fieldwork along a >100 km transect down the western margin of the Dead Sea Basin allowed Alsop and Marco (2012a) and Alsop et al. (2018) to objectively test if the orientation and geometry of slump folds within MTDs accurately reflects the orientations of paleoslopes over a regional scale. To achieve this aim, Alsop and Marco (2012a) used five different methods of slump transport analysis that provided consistent results and are typically within 15° of one another at each site. Excavation reveals the 3D geometry of slump structures, with fold hinges displaying an arc of orientations consistent with east directed movement, while thrusts display pronounced basinward vergence. Alsop and Marco (2012a) recognized that >90% of fold

hinges verge broadly toward the east, while associated axial planes generally (>90%) dip toward the west. In detail, southeast directed slumping of MTDs is recognized in the north, easterly directed transport of MTDs in the central portion, and northeast directed MTD movement at the southern end of the Dead Sea at the Peratzim locality (Figure 9.1b). The folds are typically inferred to initiate at high angles to paleoslope and verge in the flow direction. These consistent relationships support flow perturbation models in which transport-normal fold hinges are generated by layer-parallel shearing during broadly east directed slumping (Alsop and Marco, 2011, 2012a, 2012b; Alsop et al., 2016).

These studies (Alsop and Marco, 2012a; Alsop et al., 2018) form a rare regional analysis of fold data sets developed in MTDs over a regional scale and permit the recognition of a large-scale radial MTD system directed toward the depocenter of the Dead Sea. This is also supported by the studies of El-Isa and Mustafa (1986) who recognized westerly directed movement of MTDs within the Lisan Formation on the eastern margin of the basin. This radial pattern demonstrates not only the reliability of techniques to determine MTD transport but also the >90° variability of slope failure directions along the c. 100 km western margin of the Dead Sea Basin. The depositional dips (<1°) of the Lisan Formation demonstrate that local tectonics has not significantly affected the MTD transport directions with time, apart from at the Zin locality where the south-southwest directed transport is interpreted to reflect large-scale "block" tilting adjacent to the transverse Amazyahu Fault (Figure 9.1b) (Weinberger et al., 2017; Alsop et al., 2018). Thus, although MTDs within the Lisan Formation may be of slightly different (late Pleistocene) ages along the length of the Dead Sea Basin, they portray an overall coherent radial movement pattern because of the general absence of local tectonics and tilting. The gross pattern proves that the shape, and in particular the vergence, of deformed layers is governed by paleoslopes linked to MTD movement (Alsop and Marco, 2012a). The general pattern of movement is corroborated by anisotropy of magnetic susceptibility (AMS) fabrics that have been sampled from MTDs down the western margin of the Dead Sea and also display a radial pattern that mirrors the structural studies (Weinberger et al., 2017).

9.3. ANALYZING STRUCTURAL SEQUENCES DURING INTERNAL EVOLUTION OF MTDS

9.3.1. Distinguishing General Structural Sequences

A range of fold patterns and thrust geometries created during the structural evolution of MTDs can be determined from seismic sections (e.g., Frey-Martinez et al., 2005; Jolly et al., 2016; Reis et al., 2016; Cruciani et al., 2017) and outcrop studies (e.g., Lucente and Pini, 2003; Sharman et al., 2015; Ortner and Kilian, 2016; Basilone, 2017; Sobiesiak et al., 2017). Alsop and Marco (2011) recognized that the progressive evolution of folding within MTDs may be broadly categorized into initiation, translation, cessation, relaxation, and compaction phases. Folding which initiates as upright "billows" within MTDs may be progressively modified with increasing downslope directed simple shear to create asymmetric folds that develop into overturned folds, which are themselves eventually cut by downslope verging thrust systems (Alsop and Marco, 2011; Alsop et al., 2019a) (Figure 9.2a). It should be noted that the initial weak upright folds may form beyond the tip of the underlying detachment and that these early upright folds, which may partially be amplified by density variations (e.g., Alsop and Marco, 2011), are sheared over with ongoing downslope translation (Alsop et al., 2016) (Figure 9.2a–c). Meanwhile, upright folds continue to initiate at the new leading edge of the downslope propagating MTD. Therefore, the greatest deformation and most evolved structures may develop in the center of MTDs where deformation has been most protracted, rather than at downslope toes as commonly assumed (see Alsop et al., 2016).

9.3.2. Distinguishing Detailed Thrust Sequences

A range of different thrust sequences can be interpreted from both orogenic belts (e.g., Dahlstrom, 1970; Boyer and Elliot, 1982; Morley, 1988; Boyer 1992) and MTDs (e.g., de Vera et al., 2010; Ireland et al., 2011; Scarselli et al., 2016). In piggyback thrusting, new thrusts develop in the footwall of existing thrusts, potentially resulting in a back-steepening and rotation of the older thrust and an overall forward propagating system of thrusts down the slope (Figures 9.2d, 9.3a–d, and 9.4a). Some thrusts are back-rotated through the vertical so that hanging wall sequences become inverted. Examples of piggyback thrusting have been observed and interpreted from MTDs within the Peratzim study area of the Dead Sea Basin (Alsop et al., 2017a) (Figure 9.2d–f).

In an overstep (or "breakback") sequence of thrusts, new thrusts form in the hanging wall of existing thrusts, resulting in a backward propagating system of thrusts (i.e., upslope in the opposite direction to thrust transport) (Alsop et al., 2018) (Figure 9.3b–f). In addition, new thrusts may cut through existing thrusts in their footwall, resulting in re-imbrication of the sequence in an overall upslope direction. Examples of overstep thrusting have been observed and interpreted from MTDs within the Zin study area of the Dead Sea Basin (Alsop et al., 2018) (Figures 9.1b and 9.4b). Synchronous thrusting develops where more than one thrust moves at the same time and

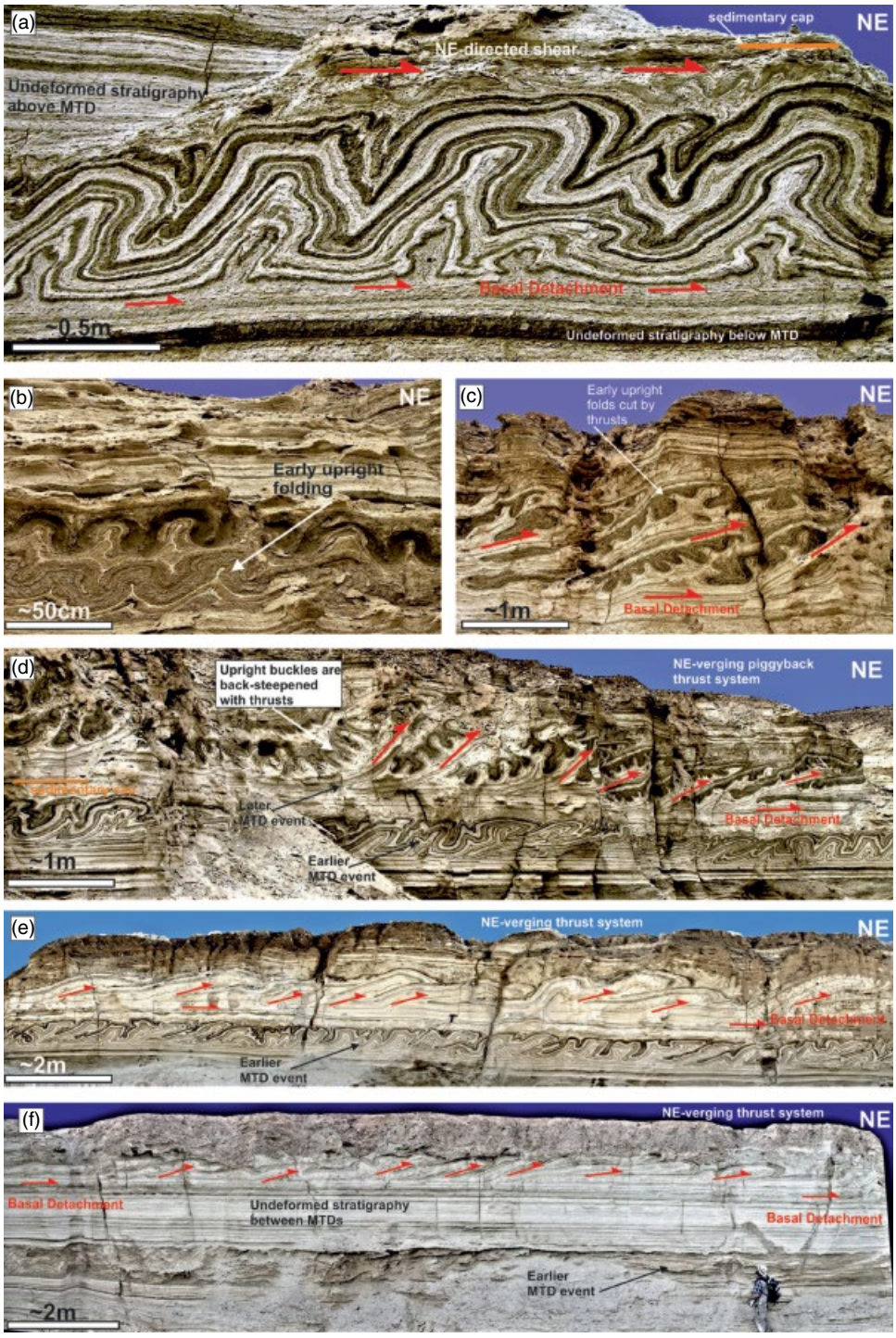

Figure 9.2 Photographs of folds and thrusts developed within MTDs of the Lisan Formation at Peratzim (N31°0449.6 E35°2104.2) (see Figure 9.1b for location). (a) Upright folds above a basal detachment that display northeast directed vergence and shear toward the basin. (b) Early upright "billow" folds that are subsequently carried on northeast verging thrusts (c). (d) Piggyback thrust sequence results in older thrusts (and the "billow" folds they carry) being progressively back-steepened. (e) Earlier (lower) MTD event dominated by folding, overlain by a northeast verging thrust system within a younger MTD. (f) Distinct northeast verging thrust system above a basal detachment that separates the MTD from undeformed stratigraphy below.

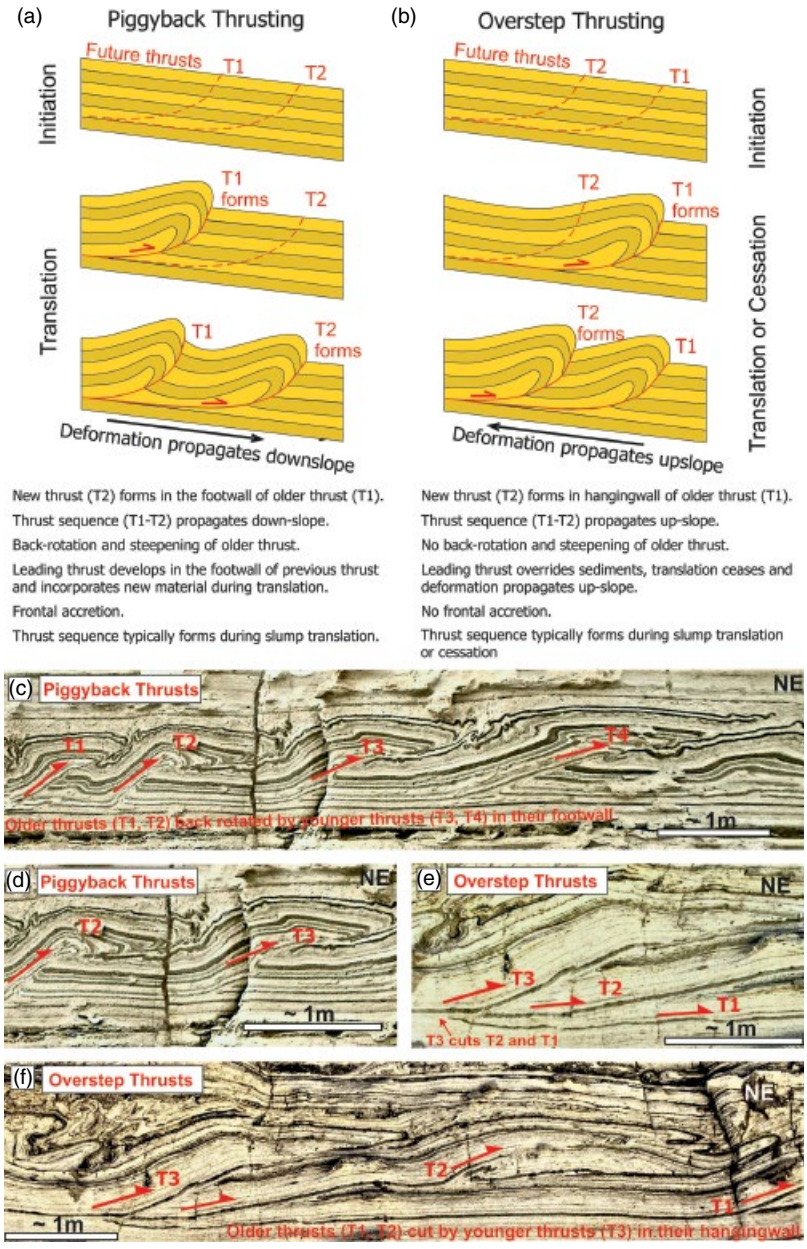

Figure 9.3 Summary cartoons of (a) piggyback thrust sequences versus (b) overstep thrust sequences. The schematic drawings show where future thrusts (T) may form during MTD initiation and their subsequent development in the translation and cessation phases of MTD movement. Text highlights the main differences between the two sequences and the direction of thrust propagation. (c) Example of piggyback thrusting from Peratzim, with (d) showing enlarged detail, where older thrusts (T1, T2) are back-steepened by younger thrusts (T3, T4) forming beneath them. (e) Example of overstep thrusting from Peratzim, with (f) showing enlarged detail, where older thrusts (T1, T2) are cut by younger thrusts (T3) forming above them.

may be supported by (a) systematic increases in displacement across older imbricates in the thrust system, whereby older thrusts continue to move and therefore accumulate the greatest displacement, and (b) bridging "shortcut" faults that develop below folded detachments (Alsop et al., 2018). Backthrusts that are truncated by forethrusts become immediately inactive and therefore display less displacement during synchronous thrusting (Figure 9.4b). In addition, oversteepened back thrusts indicate that basinward directed movement continued upslope of the backthrusts, and this suggests synchronous movement (e.g., Alsop et al., 2017b). Based on modeling, Liu and Dixon (1995, p. 885) note that "early formed thrusts continue to accumulate displacement even while new ones are

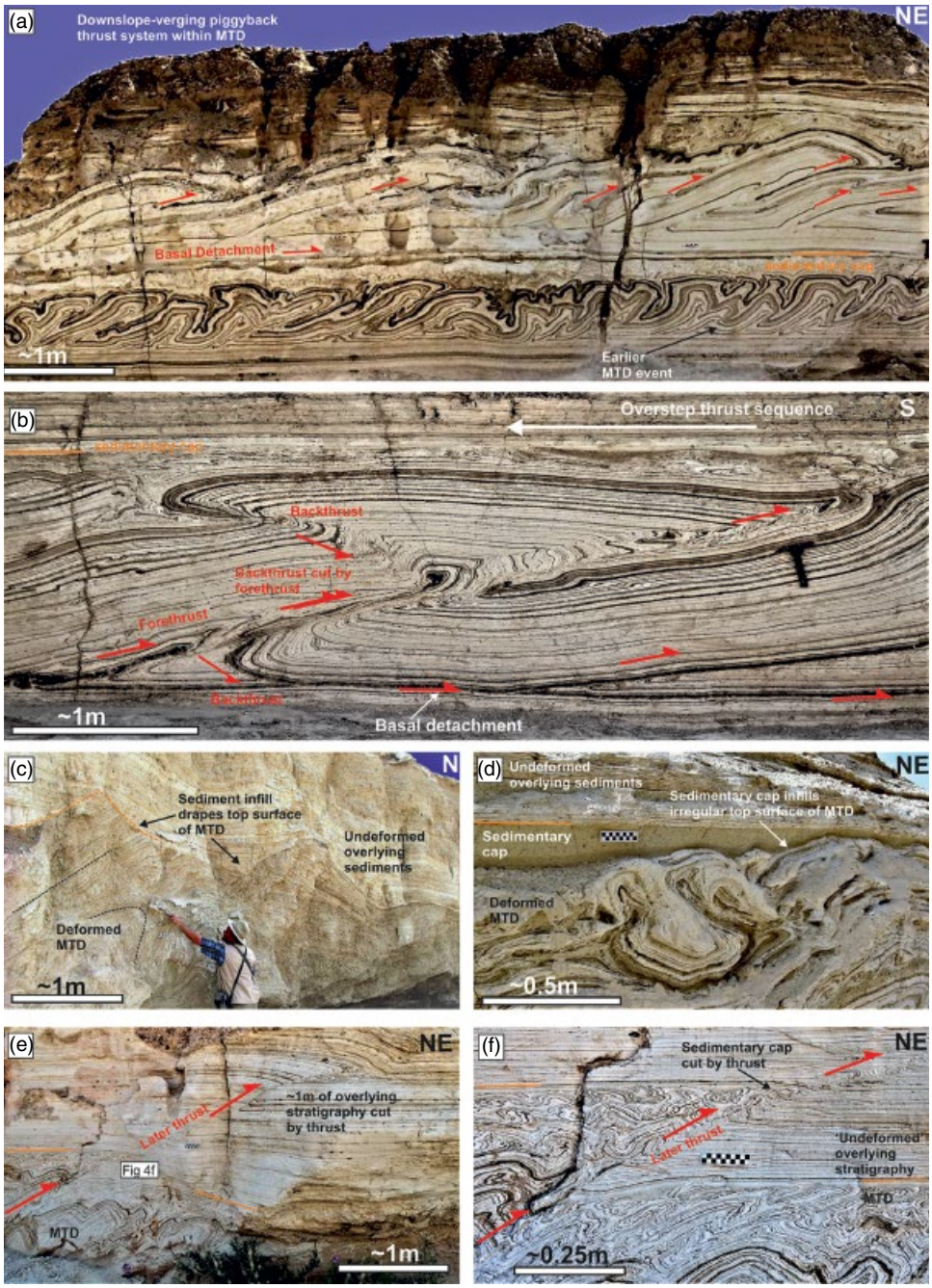

Figure 9.4 Photographs of folds and thrusts developed within MTDs of the Lisan Formation. (a) Earlier MTD event dominated by folding, overlain by a northeast verging piggyback thrust system within a younger MTD at Peratzim (refer to Figure 9.2e). (b) Southerly directed forethrust that cuts an older, underlying backthrust to define an overstep thrust sequence at Zin (N31.00615, E35.26342) (see Figure 9.1b for location). (c) Example of infilling of MTD top surface topography by later sedimentation at Almog (N31°4751.8 E35°2715.3) (see Figure 9.1b for location). (d) Sedimentary "cap" that infills the irregular top surface of the underlying and folded MTD at Peratzim. (e, f) Later thrust that cuts an MTD, together with ~1 m of overlying stratigraphy at Peratzim. The close-up photograph (f) clearly shows the younger thrust displacing the sedimentary cap, demonstrating that it represents a later "event" associated with reworking of the MTD.

nucleating." Thus, strict piggyback or overstep sequences are not necessarily supported by modeling studies, and a more relaxed approach to thrust sequencing may be required.

Analysis of larger-scale MTDs is generally based on seismic analysis, with Jolly et al. (2016, p. 74) describing a 40 km transect from the deepwater Niger delta and noting that "there is no evidence for simple forward-propagating (or piggyback) thrusting as is often predicted for fold and thrust belts." This corroborates earlier work by Corredor et al. (2005) from the same area who used stratigraphic relationships to suggest that forward propagation (piggyback), backward propagation, and coeval thrusting could all develop.

If thrusts develop during translation of the MTDs, then both piggyback and overstep sequences may form (Figure 9.3a, b). The development of piggyback thrust sequences during the translation of the MTD is different to previous models, which suggested that thrusts were generated much later during cessation of movement (e.g., Farrell, 1984; Strachan, 2008) and involve an overstep sequence as contraction propagates back upslope through the MTD (Alsop and Marco, 2011). Conversely, thrusting which forms during cessation of downslope movement generates contractional strain that propagates back up the slope from the toe and will therefore only generate overstep or out-of-sequence thrusts that will still typically verge downslope toward the basin (Alsop et al., 2018).

9.4. ANALYZING REWORKING TRIGGERED BY MULTIPLE SEISMIC EVENTS WITHIN INDIVIDUAL MTDS

A number of separate MTD horizons are observed within the Lisan Formation indicating several discrete failure "events." This deformation is considered to be triggered by earthquakes associated with seismicity along the Dead Sea Fault. Each individual MTD horizon within the Dead Sea Basin is overlain by a sedimentary "cap" deposited out of suspension following the seismically triggered failure event (Figure 9.4c, d). These "mixed" detrital and aragonite units, which may be up to 30 cm thick, comprise mud, silt, sand, and millimeter-scale fragments that infill irregularities along the top surface of the underlying MTD (Alsop et al., 2019) (Figure 9.4d). They immediately postdate the failure event that created the MTD and therefore form a natural "bounding surface" that separate the deformed sediments below from overlying non-deformed horizons. Sedimentary caps are not therefore deformed by the underlying MTD event that created them.

However, sedimentary caps may be reworked by later deformation associated with subsequent seismic events, suggesting that individual MTDs may hide more than one seismic event (Alsop et al., 2016). In some cases within the Lisan Formation, later thrusts cut the cap, and together with a further ~1 m of overlying stratigraphy, comprising aragonite-rich laminae that are deposited at a rate of ~1 mm/year (Prasad et al., 2009) (Figure 9.4e, f). New deformation that significantly postdates the underlying MTD cannot be directly associated with aftershocks or "settling" linked to the original earthquake and therefore represent multiple failure events within the individual MTD. Furthermore, MTDs that have previously been shown to be created by a double seismic event are generally thicker and marked by a greater downslope translation, compared to the immediately overlying and underlying MTDs (Alsop et al., 2016). Thus, some MTDs may conceal more than one seismic event, meaning that simple counting of deformed intervals may significantly underestimate seismic recurrence intervals. The recognition that up to 10% of MTDs may be reworked by younger seismically triggered events suggests that in some cases, the seismic recurrence interval may be shorter than previously estimated (Alsop and Marco, 2011).

9.5. ANALYZING CONTRACTIONAL STRUCTURES THAT ARE HIDDEN ON SEISMIC IMAGES

Theoretically, the amount of shortening in the downslope contractional portions of MTDs should be equivalent to, and balance, the degree of extension recorded in the upslope domain (e.g., Farrell, 1984). However, seismic sections across gravity-driven fold and thrust belts forming offshore MTDs frequently do not balance, with the amount of shortening being up to 40% less than extension measured in the upslope domain (e.g., Butler and Paton, 2010). There are a number of reasons why contraction and extension may not balance within MTD systems.

Firstly, although 40% shortening is recorded within fold and thrust systems at Peratzim, there is a 10% reduction in the amount of shortening taken up by folding and thrusting along individual thrusts (Alsop et al., 2017a). This led Alsop et al. (2017a) to suggest that heterogeneous lateral compaction increases toward the surface by ~10% and is in accord with similar estimates made by Butler and Paton (2010). This may reflect the fact that sediment toward the top of the depositional pile is more susceptible to horizontal shortening and lateral compaction during MTD movement, as it originally suffered less compaction and dewatering during limited overburden loading close to the surface.

Secondly, upright folding is interpreted to be rotated along back-steepened thrusts, indicating that it represents an early phase of layer-parallel shortening that predates thrusting (Alsop and Marco, 2011; Alsop et al. 2016) (Figure 9.2c, d). These relatively small-scale contractional

structures, with amplitudes of <2 m, may be difficult to identify on seismic sections as they are below the limits of seismic resolution.

Thirdly, estimates of upslope extension may be inaccurate due to variation in the nature and lithology of sediments being deformed closer to the upslope margin. Within Peratzim, there is an increasing detrital input toward the upslope margin, due to sediment sourced from wadi flood events. It has been suggested that extension associated with MTD translation may be partially hidden within these detrital-rich units by ductile thinning and attenuation (Alsop et al., 2016).

Fourthly, normal faults within MTDs define conjugate systems that strike parallel to the dip of the paleoslope (Alsop and Marco, 2011). Such conjugate faults indicate a component of non-plane strain deformation associated with transport-normal extension. Such "out-of-plane" movement will clearly complicate (if not negate) efforts to "balance" contraction and extension along an assumed transport-parallel section. Collectively, these observations of layer-parallel compaction, early small-scale folding, variable mechanical stratigraphy, and out-of-plane movement may provide an explanation as to why some seismic sections across basin-scale MTDs fail to balance.

9.6. ANALYZING THE EXTERNAL GEOMETRY OF MTDS AROUND THE DEAD SEA BASIN

9.6.1. Do Frontally Confined or Frontally Emergent Models Best Constrain the Bulk Geometry of MTDs?

MTDs may be divided into two categories: frontally emergent, where they translate downslope over undeformed stratigraphy and typically terminate with a distinct (emergent) thrust to form surface topography, or frontally confined, where they do not overrun downslope stratigraphy and therefore fail to create significant topographic relief (Frey-Martinez et al., 2006). Within the Dead Sea Basin, the downslope toes of MTDs do not overrun undeformed strata and are not therefore frontally emergent (Alsop et al., 2016, 2018). In detail, the toes of MTDs within the Lisan Formation are marked by upright fold trains that diminish in amplitude downslope before passing directly into undeformed beds (Alsop et al., 2016) (Figure 9.5a–c). As such, they are best described as open-ended toes (a variant of frontally confined systems) in which the apparently undeformed strata form a "soft" buttress that impedes further downslope movement (Alsop et al., 2016, 2018). Given that MTDs in the Dead Sea Basin do not terminate downslope with a distinct (emergent) thrust, but rather with upright folds in a more diffuse boundary, then significant contraction and lateral compaction could be potentially missed from analysis of seismic sections through offshore MTDs.

9.6.2. Do Critical Taper Models Constrain the Bulk Geometry of MTDs?

The "critical taper" model (e.g., Davis et al., 1983; Dahlen, 1990; Koyi, 1995) is generally applied to orogenic belts, where wedges of material are driven up a gentle underlying detachment by compression acting behind a buttress during collisional tectonics. Such modeling of critical tapers has also been applied to other settings such as accretionary complexes, and its potential role in MTDs is debated (e.g., see Bilotti and Shaw, 2005; Frey-Martinez et al., 2006; Morley, 2007; Morley et al., 2011; Alsop et al., 2018). Thrusts terminate at the same upper level in MTDs of the Lisan Formation, meaning that they generally lack surface topography and do not define a critical taper. In detail, MTDs in the Lisan Formation may be traced downslope for ~500 m where they display negligible thickness variations and taper angles of just 0.19–0.38° (Alsop et al., 2016, 2017a) (Figure 9.5b). This is an order of magnitude less than angles of ~4° typically observed in accretionary complexes (e.g., Yang et al., 2016) and is considered a consequence of weak saturated sediments translating along low-friction basal detachments marked by high fluid pressures (Alsop et al., 2016, 2017a, 2017b, 2018). This pronounced weakness also results in extreme ratios of MTD thickness compared to their downslope extent, with these ratios being significantly larger than in typical accretionary complexes (Alsop et al., 2017a). In summary, the critical taper model does not adequately explain the bulk MTD geometries developed around the Dead Sea Basin.

9.6.3. Do Dislocation Models Constrain the Bulk Geometry of MTDs?

Traditional dislocation models developed by Farrell (1984), where extension (E) is focused at the head and contraction (C) in the lower toe of an MTD, although broadly applicable in many situations (e.g., Martinsen and Bakken, 1990), are perhaps a gross simplification (Figure 9.6a). If cessation of MTD movement occurred first at the upslope head, then a late extensional strain wave (E2) propagates downslope (Figure 9.6b), whereas if cessation initiates at the downslope toe, then a contractional strain wave (C2) migrates upslope (Figure 9.6c). Within the Lisan Formation, contractional folds and extensional fractures and shears are developed in close proximity and overprint one another (Alsop and Marco, 2014) (Figure 9.5d–f). These spatial and temporal interrelationships between contractional and extensional structures led Alsop and Marco (2014) to propose that individual MTDs are composed of a series of second-order dislocation or "flow" cells that allow pockets of extension and contraction to develop anywhere in the MTD (Figure 9.6d, e). This "multi-cell flow model" involves coeval second-order

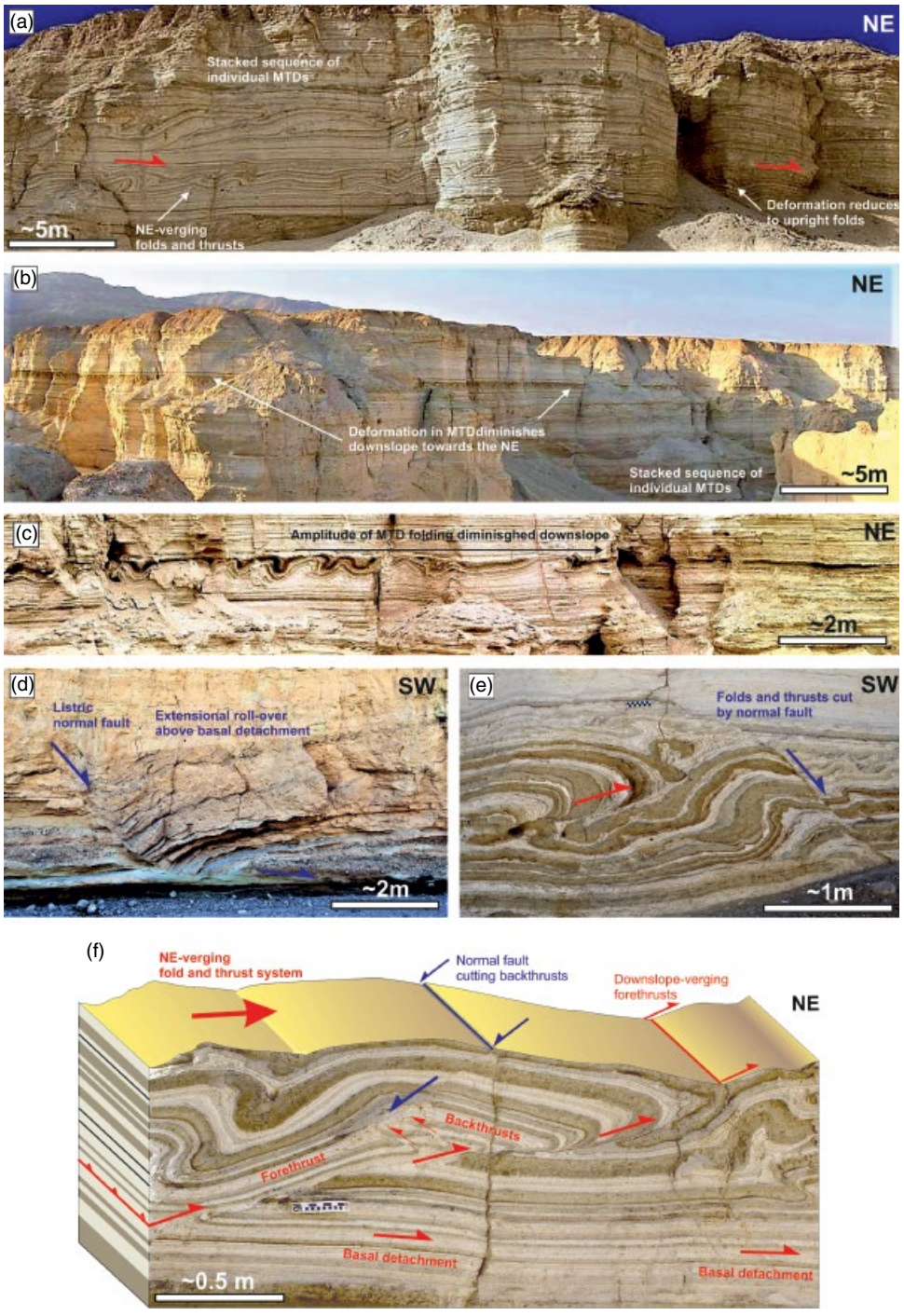

Figure 9.5 Photographs of MTDs within the Lisan Formation at Peratzim. (a, b) MTDs dying out downslope toward the NE, where we observe undeformed beds at the same stratigraphic interval. (c) Close-up photograph of inclined folds within an MTD, which diminish downslope into upright folds and eventually into relatively undeformed beds. (d) Listric fault that detaches on sands and muds within the Lisan Formation and results in extension of several meters. (e) Extensional normal fault cutting contractional folds and thrusts within a northeast translating MTD. (f) Photograph and interpreted top surface showing normal faults cutting contractional folds and thrusts.

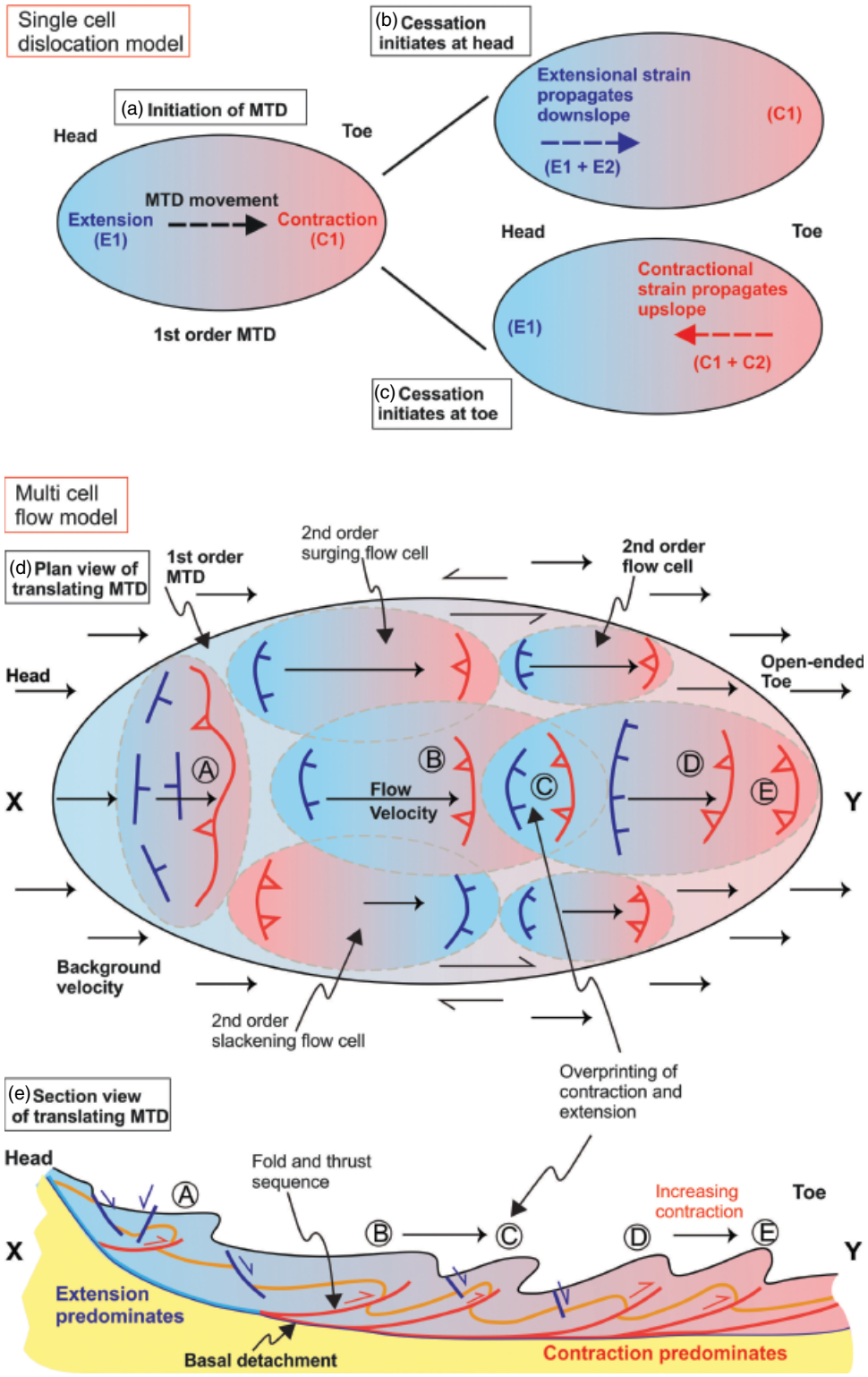

Figure 9.6 Schematic cartoon illustrating (a) the single-cell dislocation model of Farrell (1984) applied across an MTD (Source: Modified from Alsop and Marco (2014)). (a) During initiation of MTD movement, extension (E1) is concentrated at the head and contraction (C1) toward the toe of the MTD. (b) If subsequent cessation of MTD movement commences at the head, then additional extensional strain (E2) propagates downslope (broken arrow), whereas in (c), cessation initiates at the toe, resulting in additional contractional strain (C2) propagating back upslope. (d) Schematic plan view and (e) associated section view of the multi-cell flow model generated during translation of the MTD. Pockets of "surging" and "slackening" flow create second-order flow cells that interact with one another to create a range of extensional and contractional overprinting scenarios.

flow cells that interact with neighboring cells during translation of the MTD, resulting in extensional shears potentially overprinting folds (and vice versa) (Figure 9.6d, e). While the traditional single-cell dislocation model (e.g., Farrell, 1984) concentrates on structures generated during the initiation and cessation of the first-order MTD (Figure 9.6a–c), the multi-cell flow model focuses on second-order structures created during actual translation of the MTD (Figure 9.6d, e). Variations in "surging" or "slackening" flow within the MTD as it translates downslope may interact, resulting in extensional and contractional structures that are superimposed on one another in any order and in any position within the overall MTD. The strict spatial (toe and head) division of structures created during initiation and cessation of movement within traditional single-cell dislocation models is in general too simplistic and inadequate when compared to the reality observed at the outcrop scale in MTDs.

9.6.4. Do Models of Thrust Ramp Spacing Constrain the Bulk Geometry of MTDs?

The spacing between thrust ramps is defined by Liu and Dixon (1995) as the bed length between adjacent thrust ramps, when measured parallel to transport. This distance may be compared with the thickness of the stratigraphic section cut by the thrust, with Liu and Dixon (1995) noting that the spacing of thrust ramps is linearly related to the thickness of the section. Alsop et al. (2017a) noted that thicker thrust sequences are in general associated with larger thrust displacements in MTDs around the Dead Sea Basin. In detail, the average spacing of thrust ramps and the thickness of the thrust sequence in MTDs around the Dead Sea Basin display an approximate 5 : 1 ratio across a range of scales and also from piggyback sequences (e.g., Alsop et al., 2017a) and overstep sequences (e.g., Alsop et al., 2018).

These ratios are similar to those recorded in other MTDs (e.g., Gibert et al., 2005), offshore fold and thrust belts (e.g., Zalan, 2005; Butler and Paton, 2010), accretionary complexes, and orogenic belts (e.g., Morley et al., 2017). The frontally confined MTDs of the Dead Sea Basin may therefore be best interpreted using models of open-ended toes, which involve dislocation cells marked by multi-cell flow and regular thrust ramp spacing linked to bulk thickness of the MTD.

9.7. CONCLUSIONS

9.7.1. Analyzing Regional Patterns of MTD Movement Around the Dead Sea Basin

The Dead Sea Basin provides an ideal "controlled" case study where direct observations can be made at −425 m below global sea level to test the robustness of slump fold analysis to determine MTD transport directions. We have recognized a large-scale radial system of MTD movement centered on the Dead Sea depocenter. MTD transport directions vary by >90° along the ~100 km western shoreline of the Dead Sea, from southeast directed movement in the north to more northeast directed translation in the south (Figure 9.1b). This permits a better understanding of the variability that may develop in MTD movement around a modern basin. It also allows a greater appreciation of the potential complexities generated in ancient basins, where uncertainties in the paleogeographic context, together with possible later tectonics, may hide original relationships.

9.7.2. Analyzing Structural Sequences During Internal Evolution of MTDs

The progressive evolution of MTDs may be categorized into initiation, translation, cessation, relaxation, and compaction phases of deformation. Deformation may become most evolved where slope failure initiates and MTD movement commences. The implication is that many MTDs display the greatest deformation in the central area, and this diminishes toward the leading edge where MTD displacement may still be initiating. A variety of structural sequences may be observed, ranging from piggyback thrust sequences, where younger thrusts form sequentially downslope, to overstep thrust sequences, where newer thrusts propagate in an upslope direction (Figure 9.3a, b and 9.4a, b). Both of these broad sequences may themselves display aspects of synchronous thrusting, where older thrusts continue to move and therefore accrue larger displacements, while new thrusts develop. This overall variation in displacement across imbricates during synchronous thrusting may be resolvable in seismic sections and therefore represents a potential test of synchronous thrusting within large-scale MTDs.

9.7.3. Analyzing Reworking Triggered by Multiple Seismic Events Within MTDs

Individual MTDs are directly overlain by thin (up to 30 cm) sedimentary caps that are deposited out of suspension and infill relief on the MTD surface following the slope failure event. Where such sedimentary caps are themselves folded and displaced by thrusts, then subsequent deformation must have occurred (Figure 9.5e, f). Such later thrusts may also cut up to ~1 m of overlying, otherwise undeformed stratigraphy, indicating that this "event" was ~1000 years later and unrelated to aftershocks from the original failure event. Thus, outcrop studies around the Dead Sea Basin have provided detailed observations and criteria that MTDs may be reworked by

younger seismic events, meaning that in some ~10% cases, earthquake "events" may have been miscounted and the seismic recurrence interval may be shorter than realized.

9.7.4. Analyzing Contractional Structures That Are Hidden on Seismic Images

In a number of cases, contractional strain is typically found to be "missing" when attempts are made to balance large-scale structures in gravity-driven MTDs. An increase in heterogeneous lateral compaction toward water-rich sediments near the sediment surface together with upright folding that represents an early phase of layer-parallel shortening (e.g., Figure 9.2b–d) may help explain some of this contraction that is apparently not observed in seismic sections. In addition, conjugate normal faults that strike parallel to the dip of the paleoslope indicate a component of non-plane strain deformation associated with "out-of-plane" movement. This clearly complicates balancing and may help account for some of the "hidden" shortening.

9.7.5. Analyzing the External Geometry of MTDs Around the Dead Sea Basin

MTDs in the Dead Sea Basin are best described as having open-ended toes (a variant of frontally confined) in which further downslope movement is impeded by apparently undeformed strata that forms a "soft" buttress. Thrusts typically terminate at the same upper level in these MTDs, meaning that they generally lack surface topography and do not define pronounced critical tapers. As such, critical taper angles in MTDs may be an order of magnitude less than those in accretionary complexes, and the critical taper model does not therefore adequately explain the bulk MTD geometries developed around the Dead Sea Basin. Traditional dislocation models, where extension is focused at the head and contraction in the lower toe of an MTD, are a gross simplification and also not directly applicable to the Dead Sea Basin. Observations that contraction and extension may overprint one another at any positon within an MTD suggest that second-order flow cells may locally interact with one another and are linked to "pockets" of "surging" or "slackening" flow during overall downslope translation of the MTD (Figure 9.6d, e). Thrust sequences within MTDs follow established patterns, with the spacing of thrust ramps linearly related to the thickness of the section to define an approximate 5 : 1 ratio across a range of scales. In summary, the MTDs in the Lisan Formation around the Dead Sea Basin are triggered by seismic events, may be facilitated by mechanical heterogeneity linked to detrital-rich horizons, and are ultimately controlled by the paleoslope orientation.

ACKNOWLEDGMENTS

RW was supported by the Israel Science Foundation (ISF grant no. 868/17). SM acknowledges the Israel Science Foundation (ISF grant no. 1645/19). TL acknowledges the Israeli government GSI DS project 40706. We would like to thank the two anonymous reviewers and the editors for their constructive comments.

REFERENCES

Agnon, A., Migowski, C., & Marco, S. (2006). Intraclast breccia layers in laminated sequences: recorders of paleo-earthquakes. In Y. Enzel, A. Agnon, & M. Stein (Eds.), *New frontiers in Dead Sea paleoenvironmental research, Geological Society of America Special Publication* (pp. 195–214). Boulder, CO: Geological Society of America.

Almagor, G., & Garfunkel, Z. (1979). Submarine slumping in continental margin of Israel and Northern Sinai. *American Association of Petroleum Geologists Bulletin*, *63*, 324–340.

Alsop, G. I., & Marco, S. (2011). Soft-sediment deformation within seismogenic slumps of the Dead Sea Basin. *Journal of Structural Geology*, *33*, 433–457.

Alsop, G. I., & Marco, S. (2012a). A large-scale radial pattern of seismogenic slumping towards the Dead Sea Basin. *Journal of the Geological Society*, *169*, 99–110.

Alsop, G. I., & Marco, S. (2012b). Tsunami and seiche-triggered deformation within offshore sediments. *Sedimentary Geology*, *261*, 90–107.

Alsop, G. I., & Marco, S. (2013). Seismogenic slump folds formed by gravity-driven tectonics down a negligible subaqueous slope. *Tectonophysics*, *605*, 48–69.

Alsop, G. I., & Marco, S. (2014). Fold and fabric relationships in temporally and spatially evolving slump systems: A multicell flow model. *Journal of Structural Geology*, *63*, 27–49.

Alsop, G. I., Marco, S., Levi, T., & Weinberger, R. (2017a). Fold and thrust systems in Mass Transport Deposits. *Journal of Structural Geology*, *94*, 98–115.

Alsop, G. I., Marco, S., Weinberger, R., & Levi, T. (2016). Sedimentary and structural controls on seismogenic slumping within Mass Transport Deposits from the Dead Sea Basin. *Sedimentary Geology*, *344*, 71–90.

Alsop, G. I., Marco, S., Weinberger, R., & Levi, T. (2017b). Upslope-verging back thrusts developed during downslope-directed slumping of mass transport deposits. *Journal of Structural Geology*, *100*, 45–61.

Alsop, G. I., Weinberger, R., & Marco, S. (2018). Distinguishing thrust sequences in gravity-driven fold and thrust belts. *Journal of Structural Geology*, *109*, 99–119.

Alsop, G. I., Weinberger, R., Marco, S., & Levi, T. (2019). Identifying soft-sediment deformation in rocks. *Journal of Structural Geology*, 125, 248–255. https://doi.org/10.1016/j.jsg.2017.09.001

Alsop, G.I., Weinberger, R., Marco, S., Levi, T. (2019a). Folding during soft-sediment deformation. Geological Society Special Publication, Bond, C.E. and Lebit, H.D. (Editors) Folding

and fracturing of rocks: 50 years since the seminal text book of J.G. Ramsay. doi.org/10.1144/SP487.1.

Arkin, Y., & Michaeli, L. (1986). The significance of shear strength in the deformation of laminated sediments in the Dead Sea area. *Israel Journal of Earth Sciences*, *35*, 61–72.

Basilone, L. (2017). Seismogenic rotational slumps and translational glides in pelagic deep-water carbonates. Upper Tithonian-Berriasian of Southern Tethyan margin (W Sicily, Italy). *Sedimentary Geology*, *356*, 1–14.

Begin, Z. B., Ehrlich, A., & Nathan, Y. (1974). *Lake Lisan, the Pleistocene precursor of the Dead Sea, Geological Survey of Israel Bulletin* (Vol. 63, pp. 30). Jerusalem, Israel: Geological Survey of Israel.

Bilotti, F., & Shaw, J. H. (2005). Deep-water Niger Delta fold and thrust belt modeled as a critical taper wedge: The influence of elevated basal fluid pressure on structural styles. *American Association of Petroleum Geologists Bulletin*, *89*, 1475–1491.

Boyer, S. E. (1992). Geometric evidence for synchronous thrusting in the southern Alberta and northwest Montana thrust belts. In K. McClay (Ed.), *Thrust tectonics* (pp. 377–390). London: Chapman and Hall.

Boyer, S. E., & Elliot, D. (1982). Thrust systems. *American Association of Petroleum Geologists Bulletin*, *66*, 1196–1230.

Butler, R. W. H., & Paton, D. A. (2010). Evaluating lateral compaction in deepwater fold and thrust belts: How much are we missing from "nature's sandbox"? *GSA Today*, *20*, 4–10. https://doi.org/10.1130/GSATG77A.1

Corredor, F., Shaw, J. H., & Bilotti, F. (2005). Structural styles in the deep-water fold and thrust belts of the Niger Delta. *American Association of Petroleum Geologists Bulletin*, *89*, 753–780.

Cruciani, F., Barchi, M. R., Koyi, H. A., & Porreca, M. (2017). Kinematic evolution of a regional-scale gravity-driven deep-water fold-and-thrust belt: The Lamu Basin case-history (East Africa). *Tectonophysics*, *712–713*, 30–44.

Dahlen, F. A. (1990). Critical taper model of fold- and thrust-belts and accretionary wedges. *Annual Reviews Earth Planetary Science*, *18*, 55–99.

Dahlstrom, C. D. A. (1970). Structural geology in the eastern margin of the Canadian Rocky Mountains. *Bulletin of Canadian Petroleum Geology*, *18*, 332–406.

Davis, D., Suppe, J., & Dahlen, F. A. (1983). Mechanics of fold-and-thrust belts and accretionary wedges. *Journal of Geophysical Research*, *88*(B2), 1153–1172.

de Vera, J., Granado, P., & McClay, K. (2010). Structural evolution of the Orange Basin gravity-driven system, offshore Namibia. *Marine and Petroleum Geology*, *27*, 223–237.

El-Isa, Z. H., & Mustafa, H. (1986). Earthquake deformations in the Lisan deposits and seismotectonic implications. *Geophysical Journal of the Royal Astronomical Society*, *86*, 413–424.

Farrell, S. G. (1984). A dislocation model applied to slump structures. *Ainsa Basin, South Central Pyrenees, Journal of Structural Geology*, *6*, 727–736.

Field, M. E., Gardner, J. V., Jennings, A. E., & Edwards, B. D. (1982). Earthquake-induced sediment failures on a 0.25° slope, Klamath River delta, California. *Geology*, *10*, 542–546.

Frey-Martinez, J., Cartwright, J., & Hall, B. (2005). 3D seismic interpretation of slump complexes: examples from the continental margin of Israel. *Basin Research*, *17*, 83–108.

Frey-Martinez, J., Cartwright, J., & James, D. (2006). Frontally confined versus frontally emergent submarine landslides: A 3D seismic characterisation. *Marine and Petroleum Geology*, *23*, 585–604.

Garcia-Tortosa, F. J., Alfaro, P., Gibert, L., & Scott, G. (2011). Seismically induced slump on an extremely gentle slope (<1°) of the Pleistocene Tecopa paleolake (California). *Geology*, *39*, 1055–1058.

Garfunkel, Z. (1981). Internal structure of the Dead Sea leaky transform (rift) in relation to plate kinematics. *Tectonophysics*, *80*, 81–108.

Garfunkel, Z. (2014). Lateral motion and deformation along the Dead Sea Transform. In Z. Garfunkel, Z. Ben-Avraham, & E. Kagan (Eds.), *Dead Sea transform fault system: Reviews* (pp. 109–150). Dordrecht, The Netherlands: Springer. https://doi.org/10.1007/978-94-017-8872-4

Gibert, L., Sanz de Galdeano, C., Alfaro, P., Scott, G., & Lopez Garrido, A. C. (2005). Seismic-induced slump in Early Pleistocene deltaic deposits of the Baza Basin (SE Spain). *Sedimentary Geology*, *179*, 279–294.

Gladkov, A. S., Lobova, E. U., Deev, E. V., Korzhenkov, A. M., Mazeika, J. V., Abdieva, S. V., et al. (2016). Earthquake-induced soft-sediment deformation structures in Late Pleistocene lacustrine deposits of Issyk-Kul lake (Kyrgyzstan). *Sedimentary Geology*, *344*, 112–122.

Haase-Schramm, A., Goldstein, S. L., & Stein, M. (2004). U-Th dating of Lake Lisan aragonite (late Pleistocene Dead Sea) and implications for glacial East Mediterranean climate change. *Geochimica et Cosmochimica Acta*, *68*, 985–1005.

Haliva-Cohen, A., Stein, M., Goldstein, S. L., Sandler, A., & Starinsky, A. (2012). Sources and transport routes of fine detritus material to the Late Quaternary Dead Sea Basin. *Quaternary Science Reviews*, *50*, 55–70.

Ireland, M. T., Davies, R. J., Goulty, N. R., & Moy, D. J. (2011). Thick slides dominated by regular-wavelength folds and thrusts in biosiliceous sediments on the Vema Dome offshore of Norway. *Marine Geology*, *289*, 34–45.

Jablonska, D., Di Celma, C., Tondi, E., & Alsop, G. I. (2018). Internal architecture of mass-transport deposits in basinal carbonates: A case study from southern Italy. *Sedimentology*, *65*, 1246–1276. https://doi.org/10.1111/sed.12420

Jolly, B. A., Lonergan, L., & Whittaker, A. C. (2016). Growth history of fault-related folds and interaction with seabed channels in the toe-thrust region of the deep-water Niger delta. *Marine and Petroleum Geology*, *70*, 58–76.

Kagan, E., Stein, M., & Marco, S. (2018). Integrated palaeoseismic chronology of the last glacial Lake Lisan: From lake-margin seismites to deep-lake mass transport deposits. *Journal of Geophysical Research: Solid Earth*, *123*, 2806–2824. https://doi.org/10.1002/2017jB014117

Korneva, I., Tondi, E., Jablonska, D., Di Celma, C., Alsop, I., & Agosta, F. (2016). Distinguishing tectonically- and gravity-driven synsedimentary deformation structures along the Apulian platform margin (Gargano Promontory, southern Italy). *Marine and Petroleum Geology*, *73*, 479–491.

Koyi, H. (1995). Mode of internal deformation in sand wedges. *Journal of Structural Geology*, *17*, 293–300.

Lewis, K. B. (1971). Slumping on a continental slope inclined at 1-4°. *Sedimentology*, *16*, 97–110.

Liu, S., & Dixon, J. M. (1995). Localization of duplex thrust-ramps by buckling: Analog and numerical modelling. *Journal of Structural Geology*, *17*, 875–886.

Lu, Y., Waldmann, N., Alsop, G. I., & Marco, S. (2017). Interpreting soft sediment deformation and mass transport deposits as seismites in the Dead Sea depocentre. *Journal of Geophysical Research: Solid Earth*, *122*(10), 8305–8325. https://doi.org/10.1002/2017JB014342

Lucente, C. C., & Pini, G. A. (2003). Anatomy and emplacement mechanism of a large submarine slide within a Miocene foredeep in the northern Appenines, Italy: A field perspective. *American Journal of Science*, *303*, 565–602.

Marco, S., Stein, M., Agnon, A., & Ron, H. (1996). Long term earthquake clustering: a 50,000 year paleoseismic record in the Dead Sea Graben. *Journal of Geophysical Research*, *101*, 6179–6192.

Martinsen, O. J., & Bakken, B. (1990). Extensional and compressional zones in slumps and slides in the Namurian of County Claire, Eire. *Journal of the Geological Society, London*, *147*, 153–164.

Morley, C. K. (1988). Out-of-sequence thrusts. *Tectonics*, *7*, 539–561.

Morley, C. K. (2007). Interaction between critical wedge geometry and sediment supply in a deepwater fold belt, NW Borneo. *Geology*, *35*, 139–142.

Morley, C. K., King, R., Hillis, R., Tingay, M., & Backe, G. (2011). Deepwater fold and thrust belt classification, tectonics, structure and hydrocarbon prospectivity: A review. *Earth Science Reviews*, *104*, 41–91.

Morley, C. K., von Hagke, C., Hansberry, R. L., Collins, A. S., Kanitpanyacharoen, W., & King, R. (2017). Review of major shale-dominated detachment and thrust characteristics in the diagenetic zone: Part I, meso- and macro-scopic scale. *Earth-Science Reviews*, *173*, 168–228.

Nuriel, P., Weinberger, R., Kylander-Clark, A. R. C., Hacker, B. R., & Cradock, J. P. (2017). The onset of the Dead Sea transform based on calcite age-strain analyses. *Geology*, *45*, 587–590.

Ortner, H., & Kilian, S. (2016). Sediment creep on slopes in pelagic limestones: Upper Jurassic of Northern Calcareous Alps, Austria. *Sedimentary Geology*, *344*, 350–363.

Owen, G. (1996). Experimental soft-sediment deformation: Structures formed by the liquefaction of unconsolidated sands and some ancient examples. *Sedimentology*, *43*, 279–293.

Prasad, S., Negendank, J. F. W., & Stein, M. (2009). Varve counting reveals high resolution radiocarbon reservoir age variations in palaeolake Lisan. *Journal of Quaternary Science*, *24*, 690–696.

Reis, A. T., Araújo, E., Silva, C. G., Cruz, A. M., Gorini, C., Droz, L., et al. (2016). Effects of a regional décollement level for gravity tectonics on late Neogene to recent large-scale slope instabilities in the Foz do Amazonas Basin, Brazil. *Marine and Petroleum Geology*, *75*, 29–52.

Scarselli, N., McClay, K., & Elders, C. (2016). Seismic geomorphology of Cretaceous megaslides offshore Namibia (Orange Basin): Insights into segmentation and degradation of gravity-driven linked systems. *Marine and Petroleum Geology*, *75*, 151–180.

Shani-Kadmiel, S., Tsesarsky, M., Louie, J. N., & Gvirtzman, Z. (2014). Geometrical focusing as a mechanism for significant amplification of ground motion in sedimentary basins: Analytical and numerical study. *Bulletin of Earthquake Engineering*, *12*, 607–625.

Sharman, G. R., Graham, S. A., Masalimova, L. U., Shumaker, L. E., & King, P. R. (2015). Spatial patterns of deformation and palaeoslope estimation within the marginal and central portions of a basin-floor mass-transport deposit, Taranaki Basin, New Zealand. *Geosphere*, *11*, 266–306.

Sneh, A., & Weinberger, R. (2014). *Major structures of Israel and Environs, Scale 1:50,000*. Jerusalem, Israel: Israel Geological Survey.

Sobiesiak, M., Alsop, G. I., Kneller, B. C., & Milana, J. P. (2017). Sub-seismic scale folding and thrusting within an exposed mass transport deposit: A case study from NW Argentina. *Journal of Structural Geology*, *96*, 176–191.

Strachan, L. J. (2008). Flow transformations in slumps: A case study from the Waitemata Basin, New Zealand. *Sedimentology*, *55*, 1311–1332.

Weinberger, R., Levi, T., Alsop, G. I., & Eyal, Y. (2016). Coseismic horizontal slip revealed by sheared clastic dikes in the Dead Sea basin. *Geological Society of America Bulletin*, *128*, 1193–1206.

Weinberger, R., Levi, T., Alsop, G. I., & Marco, S. (2017). Kinematics of Mass Transport Deposits revealed by magnetic fabrics. *Geophysical Research Letters*, *44*, 7743–7749.

Wells, J. T., Prior, D. B., & Coleman, J. M. (1980). Flowslides in muds on extremely low angle tidal flats, northeastern South America. *Geology*, *8*, 272–275.

Woodcock, N. H. (1976a). Ludlow Series slumps and turbidites and the form of the Montgomery Trough, Powys, Wales. *Proceedings of the Geologists Association*, *87*, 169–182.

Woodcock, N. H. (1976b). Structural style in slump sheets: Ludlow Series, Powys, Wales. *Journal of the Geological Society, London*, *132*, 399–415.

Woodcock, N. H. (1979). The use of slump structures as palaeoslope orientation estimators. *Sedimentology*, *26*, 83–99.

Yang, C. M., Dong, J. J., Hsieh, Y. L., Liu, H. H., & Liu, C. L. (2016). Non-linear critical taper model and determination of accretionary wedge strength. *Tectonophysics*, *692*, 213–226.

Zalan, P. V. (2005). End members of gravitational fold and thrust belts (GFTBs) in the deep waters of Brazil. In J. H. Shaw, C. Connors, & J. Suppe (Eds.), *Seismic interpretation of contractional fault-related folds. American Association of Petroleum Geologists, Seismic Atlas, AAPG Studies in Geology* (Vol. 53, pp. 147–156). Tulsa, OK: The American Association of Petroleum Geologists.